Hindawi Publishing Corporation
Journal of Geological Research
Volume 2014, Article ID 314214, 17 pages
http://dx.doi.org/10.1155/2014/314214

Research Article

Mineralogical and Geochemical Characterization of Gold Bearing Quartz Veins and Soils in Parts of Maru Schist Belt Area, Northwestern Nigeria

Samson Adeleke Oke,[1] Akinlolu Festus Abimbola,[2] and Dieter Rammlmair[3]

[1] *Department of Geology, Federal University of Technology, Minna, Nigeria*
[2] *Department of Geology, University of Ibadan, Nigeria*
[3] *Federal Institute for Geosciences and Natural Resources (BGR), Hannover, Germany*

Correspondence should be addressed to Samson Adeleke Oke; saoke@futminna.edu.ng

Received 30 November 2013; Revised 18 April 2014; Accepted 26 May 2014; Published 14 July 2014

Academic Editor: Teresa Moreno

Epigenetic, N-S, NNE-SSW quartz veins crosscut metapelites and metagabbro in Maru area. The objectives of this work were to study field, mineralogy, and geochemical characteristics of gold bearing quartz veins and soils. Euhedral and polygonal magnetite with hematite constituted the major ore minerals. Quartz occurred as main gangue phase with appreciable sericite and chlorite. The mineralogy of soil retrieved from twelve minor gold fields examined with X-ray diffraction is quartz ± albite ± microcline ± muscovite ± hornblende ± magnetite ± illite ± kaolinite ± halloysite ± smectite ± goethite ± vermiculite ± chlorite. The concentration of gold in quartz vein varies from 10.0 to 6280.0 ppb with appreciable Pb (3.5–157.0 ppm) and ΣREE (3.6 to 82.9 ppm). Gold content in soil varies from < 5.0 to 5700.0 ppb. The soil is characterized by As ± Sb gold's pathfinder geochemical association. Multidata set analysis revealed most favourable areas for gold. Possibility of magmatic fluids as part of ore constituents is feasible due to presence of several intrusions close to quartz veins. Based on field, mineralogical, and geochemical evidences, ore fluids may have been derived from fracturing, metamorphic dewatering, crustal devolatilization of sedimentary, gabbroic protoliths, and emplaced in an orogenic setting.

1. Introduction

Precambrian rocks within and around Maru Schist belt host some quartz veins that are gold bearing. The gold deposits were heavily mined during the colonial era approximately before 1960 and after that period by artisanal miners. General descriptive information on gold mineralization in Maru schist belt has been documented [1–3]. Gold occurs primarily in quartz veins and as placers in soil (eluvial) and stream sediments (alluvial). The quartz veins containing gold occur in association with metamorphosed rocks ranging in composition from semipelitic to pelitic and mafic. Primary gold mineralization produced chemical signature in the overburden and surrounding soil probably through weathering processes. Weathering processes provide samples (soils and stream sediments) that yield data on local hidden mineralization or on the potential existence of major or minor mineralization in a wide region. The residual soil is the geochemical sample that is often used to detect the location of hidden mineralization once a zone of economic interest is localized [4]. Migration of groundwater provided chemical response at the surface. This process produces elemental dispersion pattern [5]. Most of these dispersed elements (e.g., Cu, Ag, Zn, Cd, As, Bi, Pb, Sb, Hg, W, Mo. and Se) are useful indicators or pathfinders for the presence of gold [6, 7]. Analyses of samples taken enable the observation of patterns and concentrations in the distribution of metals in the soil which would potentially indicate enriched rock underneath.

This research examined field characteristics, mineralogical and geochemical composition of gold bearing quartz veins and soils and used the aforementioned to establish prospectivity prediction models that indicate ranking of areas

with potential gold mineralization. This is with the overall aim of using the data to discover the extension of the minor gold field vertically or laterally and assess their prospects. The possible origin of the gold bearing fluid was inferred.

2. Regional Geological Setting

Maru schist belt is a portion of basement complex of Northwestern Nigeria. It is one of the low grade, upper proterozoic, metasedimentary dominated, and metavolcanic with intrusive igneous rocks schist belt in Western Nigeria [8]. It is bounded to the East by Wonaka schist belt and to the West by Anka schist belt. The schist belts trend N-S and have been infolded into the migmatite-gneiss-quartzite complex. This complex constitutes the predominant rock group in the basement of Eburnean (about 2000 Ma) to Liberian (ca 2800 Ma) age [9].

Maru schist belt lies Northeast of the Kushaka schist belt with both having similar lithological assemblages and is approximately 200 km long and 12–19 km wide. It is linear super crustal remnants in the polycyclic basement complex of Nigeria. The contact between the schist belt and the gneiss—migmatite complex, are conformable but are locally migmatised around intrusive granitic plutons. The Maru schist belt consists predominantly of pelitic to semipelitic metasedimentary with subordinate interlayered psammites, banded iron formation (BIF) and amphibolites. All the rocks strike approximately North-South, parallel to the structural grain of the surrounding basement complex [10]. The entire Maru belt has been differentiated into Eastern and Western units [11]. While the Eastern unit consists of pelites with locally dominant quartzite and iron formations, the Western unit is almost entirely made up of pelites.

The fine-grained laminated sediments, both pelites and iron formation, indicate quiet water conditions; the predominance of iron oxides suggests oxygenated waters, although sometimes pyrite occurs, indicating anoxic conditions. Metasandstones were deposited in a higher energy environment, reflecting shallow water or increased sediment supply. The Maru schist belt contains internal plutons of granite, granodiorite, diorite, tonalite, and syenites (Figure 1).

The structure of the study area has imprints of the entire northwestern Nigerian Basement Complex which have passed through a minimum of two episodes (polyphase) of deformation [12, 13]. Three deformation episodes (D_1, D_2, and D_3) were recognized in the area investigated. The second deformation episode (D_2) is the major phase. The first (D_1) and third (D_3) deformational episodes are generally less common. The first deformation episode (D_1) produced first axial planar foliation (S_1) and first fold phase (F_1). The second deformation episode gave rise to S_2 and F_2 second axial planar foliation and fold phase, respectively. The third deformation episode (D_3) resulted from S_3 and F_3 third axial planar foliation and fold phase, respectively. Several strike slip faults have been mapped within Maru schist belt.

The quartz veins were hosted by metapelites (slate, phyllite and schist) with metagabbro. Slate and phyllite occur as low lying highly fissile rocks with diagnostic slaty and phyllitic cleavages, respectively. Schist occurs as low lying rocks with N-S trending, moderately to steeply dipping schistose planes. The metapelites displayed lepidoblastic texture. These rocks experienced low grade green schist regional metamorphism [14]. Metagabbro are porphyroblastic and have been metamorphosed to epidote amphibolite facies conditions [15].

3. Materials and Methods

Quartz veins were collected as grab samples with the use of geological hammer during structural and lithological mapping of the study area. Soil samples from B horizon (0.50–1.0 metre) were collected within the Maru schist belt and other selected parts of the study area at twelve small gold fields established by artisanal miners and local mining companies after various reconnaissance surveys. The soils were excavated with the use of stainless steel hand auger and collected directly into a polythene bag.

About one kg of soil sample was collected from each location. A total of eighteen samples were collected. The geographic coordinates of all the sampling points were determined with a Garmin global positioning system.

All the soil samples were allowed to pass through 200 μm sieve and their mineralogy subsequently was examined with the use of X-ray diffraction (XRD) technique. A Philips diffractometer PW 3710 (40 Kv, 30 mA) with Cu k_α radiation, equipped with a fixed divergence silt and a secondary graphite monochromator, was used for X-ray diffraction. Whole rock powder samples were scanned with a step size of 0.02° 2 theta (θ) and counting time of 0.5 second per step over a measuring range of 2 to 65° 2 theta (θ). X pert plus software (Philips) was used to identify the crystalline phases. Thin sections and polished slides were prepared from gold bearing quartz veins and studied under petrological microscope.

Gold bearing quartz veins and soils samples were crushed, sieved, pulverised with hardened steel, and allowed to pass through 75 μm. Thereafter, major oxide and some trace elements concentration of majority of gold bearing quartz veins collected were analysed with two wave length dispersive X ray fluorescence spectrometers (PW 1480 and PW 2400). Four quartz veins identified to contain visible gold grains were selected and analysed for gold, trace, and rare earth elements with inductively coupled plasma mass spectroscopy (ICP-MS) method. The samples were initially decomposed with HCL, HNO_3, $HCLO_4$, and HF acids in order to achieve near total digestion. The procedure followed is contained in [22]. The quartz veins that contain visible gold grains were subsequently assayed with fire assay and instrumental neutron activation analysis (INNA) in order to quantitatively determine the concentration of gold traced to international reference standards as documented in [23]. Twelve soil samples that represent each small minor gold field were analysed with instrumental neutron activation analysis (INAA) equipment for Au (gold) and twenty-two (22) elements.

Thin section preparation, X-ray diffractometry, and wavelength dispersive X ray fluorescence spectrometry were

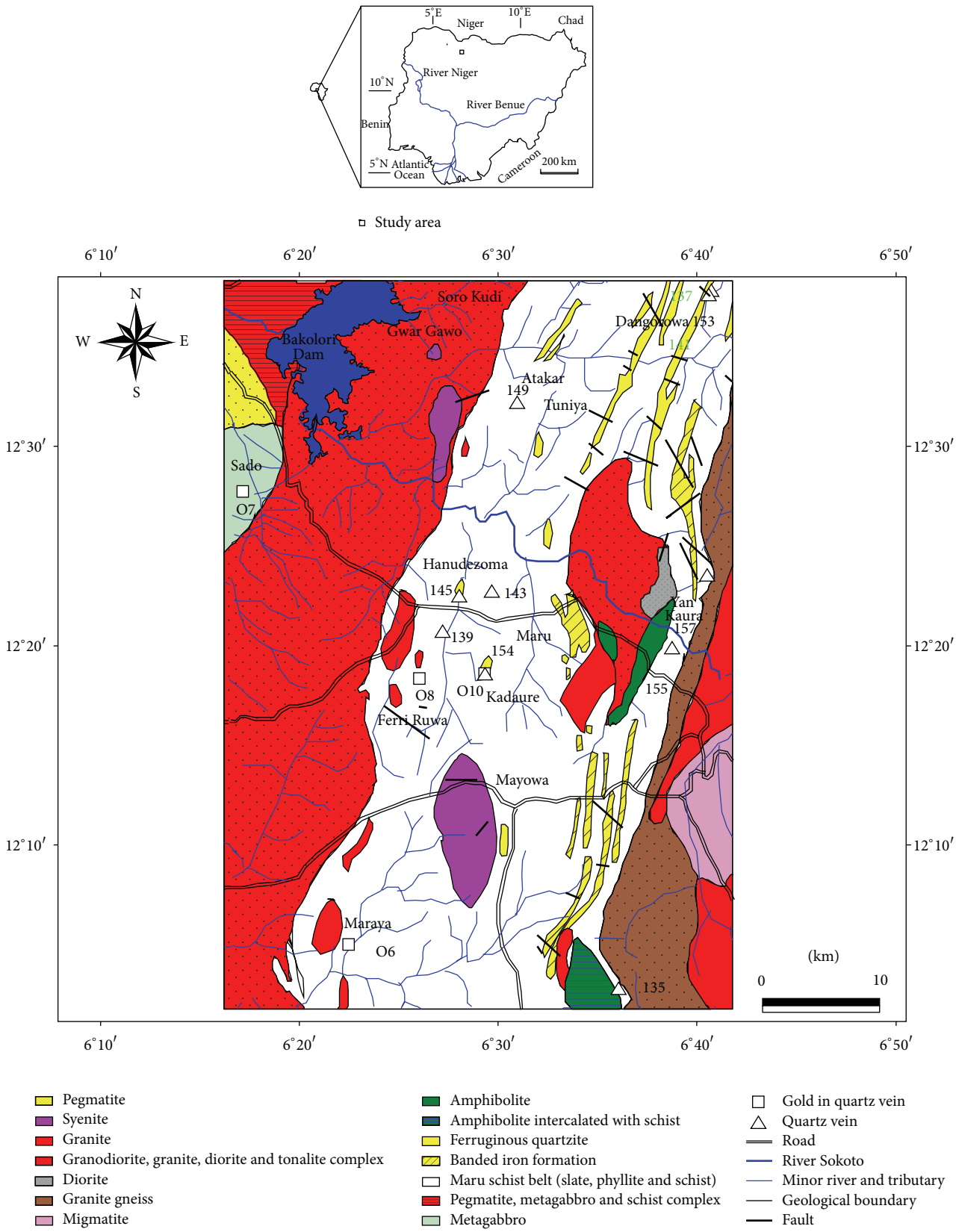

Figure 1: Geological map of the study area showing locations of gold bearing quartz veins with map of Africa and Nigeria above.

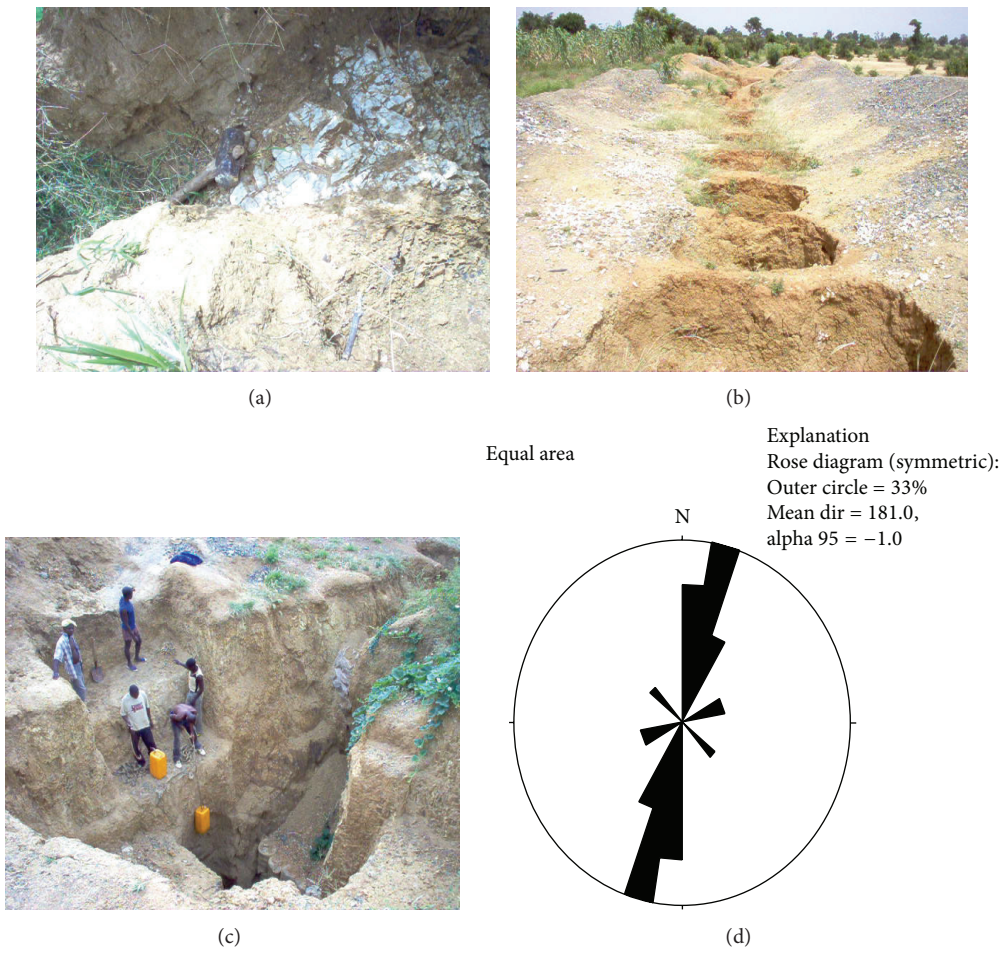

Figure 2: Illustrates quartz vein hosting primary gold in Sado (a), pits dug along the trend of quartz vein in Sado (b), excavated pit for artisanal mining of primary gold in Sado (c), and rose diagram of trend of gold bearing quartz veins within and around Maru Schist belt (d).

undertaken in the laboratory of Federal Institute for Geosciences and Natural Resources, Hannover, Germany. The polished section was carried out at Department of Geology, University of Cologne, Germany. Inductively coupled plasma-mass spectroscopy (ICP-MS) and fire assay and instrumental neutron activation analysis (INNA) were carried out at Activation Laboratory Ltd, Ancaster, Ontario, Canada.

4. Results and Discussion

4.1. Occurrence and Mineralogy of Gold Bearing Quartz Veins. Gold bearing quartz veins crosscut metapelites (slate, phyllite with schist) and metagabbro in the study area (Figure 2(a)) indicating epigenetic style of mineralization. These veins vary considerably in thickness and often exhibit significant vertical and longitudinal continuity (Figure 2(b)). Vein contacts are generally sharp and steeply dipping. These veins were identified South of Maraya, West of Sado, West of river Ferri Ruwa and East of river Ferri Ruwa. Other gold bearing quartz veins occur at Tuniya, Hanudezoma, Dangorowa, Yan Kaura and Kadaure within the area investigated (Figure 1). At Sado, sets of intersecting quartz veins containing gold that trend 170°–350°, 130°–310°, and 60°–240° have been mined by artisanal miners. Several pits were excavated along the trend of the quartz veins some to a maximum length of 96m and a recovery depth of about 23 m (Figure 2(c)). Metagabbro host the gold bearing quartz vein in Sado. Majority of the gold bearing quartz veins occur within the Maru schist belt. The quartz veins trend principally in the N-S and NNE-SSW directions. The trend is similar to the regional strike of Maru schist belt (Figure 2(d)).

Euhedral and polygonal magnetite with hematite were observed (Figure 3(a)) in the quartz veins. The replacement of magnetite by hematite due to oxidation (martitization) was clearly visible. The grey-brownish colour represents magnetite being replaced by hematite (bright white) (Figure 3(b)). The main gauge mineral in the quartz vein consists of exclusively xenomorphic quartz crystals (more than 98% in modal composition), occurring in almost equal grain sizes (equigranular). The quartz crystals that show undulatory extinction are aligned and this is due to tectonic stress. The alignment of quartz crystals also indicates deformation within a shear zone. Flaky chlorite displaying cleavage and

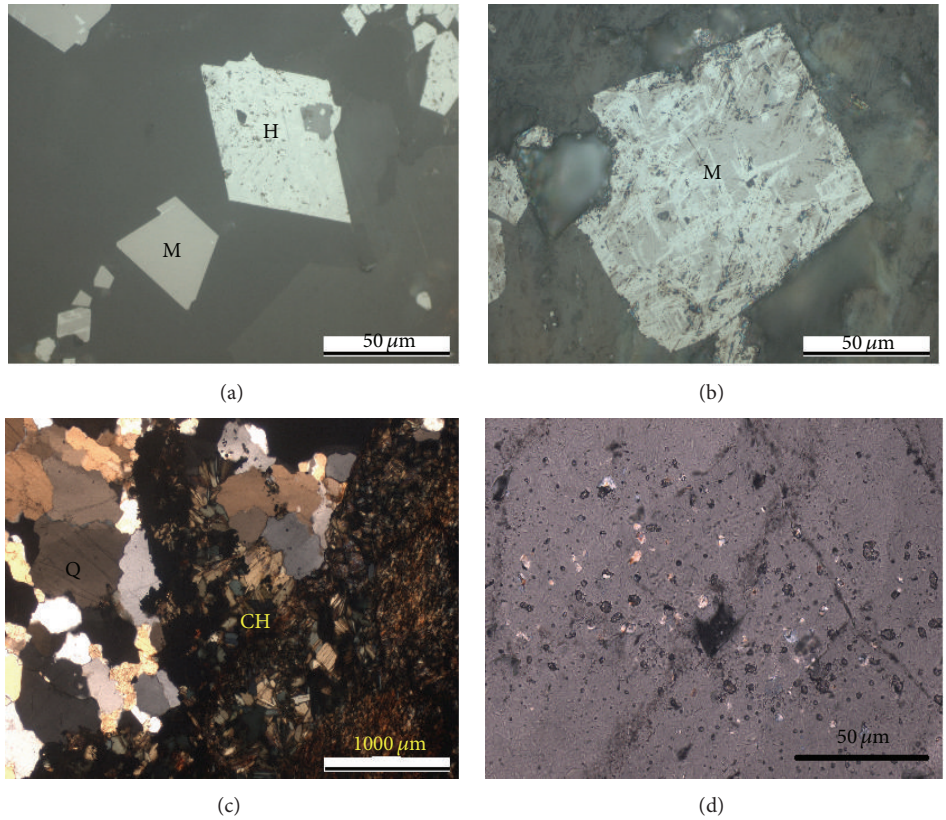

Figure 3: Photomicrograph of quartz vein in reflected cross polarized light (in air) showing euhedral isometric polygonal hematite (H) and magnetite (M) (a), isometric euhedral magnetite, displaying martitization (b). Hematite and chlorite (CH) across quartz (Q) crystals with (c) sericite and fluid inclusions (d) as observed under transmitted cross polarised light.

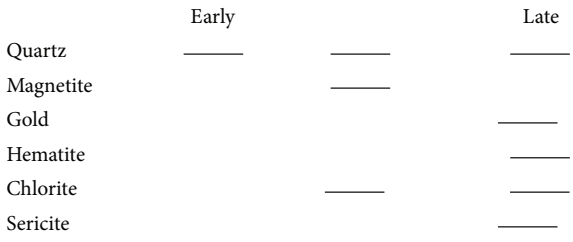

Figure 4: Summarized mineral paragenesis of quartz vein containing gold obtained from the study area.

anomalous interference colour under cross polarized light are present in some quartz veins (Figure 3(c)). Anhedral sericite and fluid inclusions are contained in the quartz crystals (Figure 3(d)).

Figure 4 summarises the mineral paragenesis of the quartz vein containing gold. The sequence comprises initial host rock formation which latter experienced fracturing. This was subsequently followed by introduction of hydrothermal mineralizing fluid composing of quartz, gold, and magnetite. Hematite replaced magnetite. Some primary minerals in the quartz veins were later altered to chlorite and sericite. Remarkable development of quartz, sericite, and chlorite alteration minerals in the quartz veins confirms that silicification, sericitization, and chlorization processes are associated with gold mineralization.

4.2. Mineralogy of Gold Bearing Soils. Eluvial gold occurs within Maru schist belt in some locations called minor gold fields and has been recovered by artisanal miners through excavation of several pits of various dimensions and depths. The soil rich in gold was panned and washed and lighter fractions were removed until heavy minerals with gold grains remained. The gold grains were separated from the heavy mineral concentrates manually. The soils were retrieved from Tuniya, Yar Kaura, Sado, Mayowa, Maru, Atakar, Hanudezoma, Gwar Gawo, Kadaure, Ferri Ruwa, Dangowa, and Soro Kudi minor gold fields (Figure 5).

The summary of the mineralogical composition of the soil sample is presented in Table 1. Residual weathering of rocks that underlain the study area resulted into soil formation and this is reflected in its mineralogy. Weathering facilitated the dispersion of the geological materials containing primary gold mineralization. The major mineralogical constituent in all the soil samples examined is quartz. There is no distinct pattern in the mineralogical composition of the minor and trace constituents. Lesser amount of albite, microcline, muscovite, hornblende, magnetite, clay minerals (illite, kaolinite,

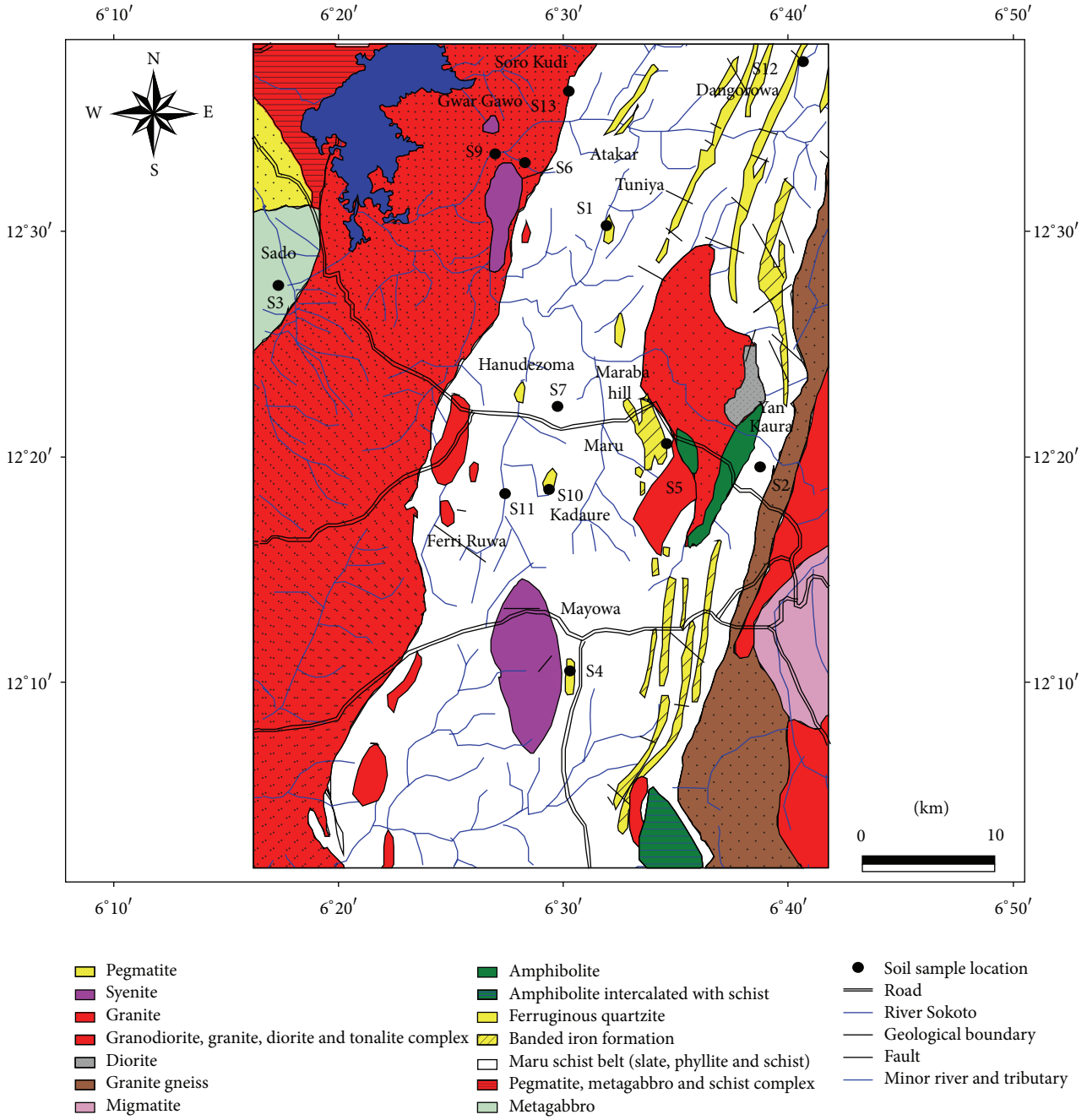

Figure 5: Geological map of the study area showing the locations of soil samples.

halloysite, smectite, goethite, vermiculite and chlorite) are present. The sources of albite are dominantly from the weathering of amphibolite, tonalite, diorite, and granodiorite that intruded Maru schist belt. Granite, migmatitic gneiss, and granite gneiss weathering liberated microcline. The origins of the clay minerals and muscovite are from the metasediments metamorphosed into metapelites (slate, phyllite, and schist) of the Maru schist belt [24]. Some of the soil samples contain hornblende as minor and trace constituents. The source of hornblende from the soil sample in Maru field is from amphibolite contained within the Maru schist belt. At Sado field, hornblende in form of riebeckite occurs as minor phase and the source is the host lithology (metagabbro) [25]. Weathering of the metasediments released significant quantity of biotite that was later altered into chlorite. Hematite occurs as trace constituent in soil sample from Maru and Hanudezoma fields and the origin is from the banded iron formation from Maraba hill within Maru schist belt [10, 26]).

4.3. Geochemistry of Gold Bearing Quartz Veins. The whole rock geochemical composition of quartz vein obtained with X-ray fluorescence method of analysis is contained in Table 2.

Table 1: Mineral composition of soil samples on the basis of XRD analysis.

S/No.	Field	Major constituent	Minor constituent	Trace constituent
307	Maru	Quartz	Smectite + vermiculite	Albite + microcline kaolinite + halloysite
259	Maru	Quartz	Albite + microcline	Muscovite + illite + kaolinite halloysite
263	Maru	Quartz + Albite	Muscovite + illite + kaolinite	Smectite + vermiculite
261	Maru	Quartz		Microcline + albite + hematite + muscovite + illite + hornblende
279	Maru	Quartz	Albite + microcline + muscovite + illite	Kaolinite + smectite + hornblende
291	Maru	Quartz		Albite + microcline
S1	Tuniya	Quartz	Muscovite + illite	Kaolinite + microcline + albite
S3	Sado	Smectite + Vermiculite Quartz + Albite	Hornblende (riebeckite)	Halloysite
S4	Mayowa	Quartz	Chlorite + muscovite + illite	Goethite + illemnite
S9	Gwar Gawo	Quartz		Albite + microcline + hornblende (riebeckite) + muscovite + illite
S11	Ferri Ruwa	Quartz	Albite + microcline	
S12	Dangowa	Quartz	Muscovite + illite + kaolinite	Goethite + albite
S13	Soro Kudi	Quartz		Albite + microcline + muscovite + illite + kaolinite
255	Hanudezoma	Quartz	Muscovite + illite + kaolinite	Goethite + hematite
267	Hanudezoma	Quartz	Muscovite + illite + kaolinite	Goethite + microcline
273	Yan Kaura	Quartz		Microcline + kaolinite
288	Atakar	Quartz		Hornblende + smectite
303	Kadaure	Quartz	Muscovite + illite	Kaolinite + goethite

The quartz veins are highly siliceous. The composition of Al_2O_3 varies from <0.05 to 13.68 wt%, Fe_2O_3 ranges from 0.07 to 6.26 wt%, Na_2O wt% is of the order of <0.01 to 3.41 wt%, and K_2O varies from 0.008 to 5.812 wt%. The concentrations of other major oxides are very low.

Negative or inverse relationship exists between TiO_2, Al_2O_3, CaO, and Fe_2O_3 with SiO_2.

Appreciable amount of Ba, Cu, Rb, and Zr up to 486 ppm, 41 ppm, 323 ppm and 111 ppm, respectively, is noteworthy. Positive relationships exist between the concentration of Fe_2O_3 versus TiO_2, Cu versus Ba, Cu versus Zn and Zn versus Zr.

The results of gold bearing quartz veins analysed with fire assay and instrumental neutron activation analysis are contained in Table 3. The concentration of gold varies from 10 to 6280 ppb and exceeded the background (5 ppb) and Clarke's concentration (4 ppb) in unmineralized materials in all the quartz veins. This signifies that the quartz veins are mineralized with gold. Samples O6 (10 ppb of gold) and O8 (12 ppb of gold) were recovered from the quartz veins that outcropped on the surface south of Maraya and west of River Ferri Ruwa, respectively. Samples O7 (6280 ppb of gold) and O10 (39 ppb) were retrieved from approximately 23.4 metres and 10.40 metres, respectively, from the existing surface. This implies that higher gold ore grade can be obtained from the subsurface (Figure 1). The concentration of gold in sample O7 (6280 ppb of gold) exceeded the minimum value (2000 ppb) to qualify as an ore. Economic occurrence of gold generally consists of very small amounts of dispersed gold or gold-silver alloys. Even in the well-known ore of the Witwatersrand in South Africa, the average concentration of gold is only about 16000 ppb [27].

The results of gold bearing quartz veins analysed with inductively coupled plasma mass spectrometry method are

Table 2: Results of whole-rock X-ray florescence analyses of quartz vein samples.

Sample number →	135	137	139	141	143	145	149	153	154	155	157	Range	Mean
Major oxide (wt.%) ↓													
SiO_2	92.22	89.81	99.24	99.22	99.68	99.23	94.56	83.54	99.43	97.49	74.25	74.25 to 99.68	93.52
TiO_2	0.014	0.052	0.003	0.005	<0.001	0.003	0.139	0.264	0.004	0.03	0.098	<0.001 to 0.264	—
Al_2O_3	2.23	1.49	0.27	0.34	<0.05	0.29	0.9	8.96	0.1	0.94	13.68	<0.05 to 13.68	—
Fe_2O_3	2.59	6.26	0.11	0.13	0.07	0.14	3.12	3.56	0.21	0.66	1.09	0.07 to 6.26	1.63
MnO	0.104	0.557	0.002	<0.001	0.002	0.002	0.084	0.03	0.002	0.04	0.008	<0.001 to 0.557	—
MgO	1.23	0.02	0.02	0.02	<0.01	0.02	0.36	1.74	0.02	0.03	0.08	<0.01 to 1.74	—
CaO	0.229	0.022	0.027	0.027	0.026	0.029	0.126	0.286	0.062	0.043	0.358	0.022 to 0.358	0.11
Na_2O	<0.01	<0.01	<0.01	<0.01	<0.01	<0.01	<0.01	0.56	<0.01	<0.01	3.41	<0.01 to 3.41	—
K_2O	0.026	0.064	0.075	0.103	0.008	0.089	0.022	0.024	0.01	0.032	5.812	0.008 to 5.812	0.57
P_2O_5	0.171	0.191	0.006	0.005	0.006	0.008	0.098	0.011	0.01	0.008	0.029	0.008 to 0.191	0.05
Cl	0.008	0.006	0.013	0.013	0.012	0.015	0.008	0.045	0.016	0.015	0.012	0.008 to 0.016	0.01
LOI	1.08	1.35	0.19	0.16	0.12	0.15	0.49	0.95	0.09	0.69	0.99	0.09 to 1.35	0.57
Total	**99.89**	**99.8**	**99.95**	**99.98**	**99.98**	**99.98**	**99.92**	**100.01**	**99.97**	**99.95**	**99.83**	**99.89 to 100.01**	**99.93**
Trace element (ppm) ↓													
As	<2	39	<2	<2	<2	<2	<2	<2	<2	<2	17	<2 to 39	—
Ba	129	251	28	13	24	32	7	5	<4	76	486	<4 to 486	—
Ce	75	59	22	<17	<17	<17	<18	<17	<17	<17	68	<17 to 68	—
Co	12	28	<3	<2	<2	<3	3	6	<3	6	<3	<3 to 28	—
Cr	<4	135	<4	<4	<4	<4	34	<4	<4	<4	<4	<4 to 135	—
Cu	12	14	5	6	6	6	41	6	6	13	25	5 to 41	12.73
Ga	4	2	<2	<2	<2	<2	2	18	<2	2	24	<2 to 24	—
Nd	62	14	<12	<12	<12	<12	<13	14	<12	<12	<13	<13 to 62	—
Ni	17	46	<2	<2	<2	<2	7	12	<2	3	<2	<2 to 46	—
Pb	3	861	6	<3	3	3	<3	6	5	5	74	<3 to 861	—
Rb	7	9	9	8	5	10	7	<2	5	9	323	<2 to 323	—
Sm	14	18	<13	<13	<13	<13	<14	22	<13	<13	<14	<14 to 18	—
Sr	36	12	<2	<2	<2	<2	8	48	<2	<2	113	<2 to 113	—
Th	9	7	7	4	6	5	12	<3	5	6	48	<3 to 48	—
V	8	30	<5	<5	<5	<5	17	76	<5	16	<6	<6 to 76	—
Y	9	4	<3	<3	<3	<3	5	12	<3	3	16	<3 to 16	—
Zn	77	26	4	4	4	2	22	76	5	7	17	2 to 77	22.18
Zr	7	16	7	4	4	5	31	28	6	11	111	4 to 111	20.91
K/Rb	3.71	7.11	0.01	12.88	0	8.9	0	12	2	3.56	17.99	0 to 17.99	6.2
K/Ba	0.2	0.25	0	7.92	0	2.78	0	4.8	2.5	0.42	11.96	0 to 11.96	2.8
Ba/Rb	18.43	27.89	3.11	1.63	4.8	3.2	1	2.5	0.8	8.44	1.5	0.80 to 27.89	6.66
Rb/Sr	0.19	0.75	4.5	4	2.5	5	0.88	0.04	2.5	4.5	2.86	0.19 to 4.50	2.52

Table 3: Results of fire assay and instrumental neutron activation analysis of gold bearing quartz veins.

Detection limit →	Au 1 pbb	Normal abundance in un-mineralized material (ppb) [a]	Clarke value (ppb) [b]	Approximate minimum quantity to qualify as an ore (ppb) [c]	Mass (g)
Sample number ↓					
O6	10	5	4	2000	30.50
O7	6280	5	4	2000	20.10
O8	12	5	4	2000	20.70
O10	39	5	4	2000	30.40

[a]: [19] and [20]; [b and c]: [21].

Table 4: Trace element of gold bearing quartz veins analysed with inductively coupled plasma mass spectrometry technique.

Sample number →	O6	O7	O8	O10	Min	Max	Mean
Trace element (ppm) ↓							
Ni	2.5	16.1	7.8	15.1	2.5	16.1	4.40
As	1	92	3.1	43.8	1	92	11.20
Sr	2.6	3.3	22.7	3.6	2.6	22.7	1.55
Ba	11	6.8	36.6	29	6.8	36.6	10
La	0.5	0.7	21.6	3.3	0.5	21.6	0.95
Ce	1.84	2.23	40.8	4.88	1.84	40.8	1.68
Cr	9.3	76.4	25.2	6.8	6.8	76.4	4.03
Pb	3.51	157	28	19.9	3.51	157	5.85
Co	0.5	23.1	4.9	56.4	0.5	56.4	14.23
Cu	15	798	16.6	156	15	798	42.75
Zn	7	544	12.5	21.9	7	544	7.23
Au	7.8	6980	26.3	26.5	7.8	6980	8.58
K	10	10	60	20	10	60	25.00
As	1	92	3.1	43.8	1	92	34.98
Ba	11	6.8	36.6	29	6.8	36.6	20.85
Rb	0.3	0.2	2.8	1.1	0.3	2.8	1.10
Sr	2.6	3.3	22.7	3.6	2.6	22.7	8.05
K/Rb	33.33	50.00	21.43	18.18	18.18	50.00	30.74
K/Ba	0.91	1.47	1.64	0.69	0.69	1.64	1.18
Ba/Rb	36.67	34.00	13.07	26.36	13.07	36.67	27.53
Rb/Sr	0.12	0.06	0.12	0.31	0.06	0.31	0.15

contained in Table 4. The quartz veins are enriched in Cu, Zn, Sr, As, Ni, Co, Pb, Cr, Ce, La, and Ba with respect to other trace and rare elements. However only the concentration of As and Pb exceeded the backgrounds in unmineralized rocks for As (5 ppm) and Pb (10 ppm) in majority of the quartz veins samples.

The results of concentrations of gold in the quartz veins obtained by inductively coupled plasma mass spectrometry technique compare favourably well with those retrieved from fire assay-neutron activation analysis instrument. The ΣREE varies from 3.15 to 82.90 ppm with notable LREE and HREE fractionation. The samples show strong LREE/HREE fractionation with $(La/Yb)_n$ ranges from 2 to 36. Figure 6 illustrates the chondrite normalized plots of rare earth element [16] in gold bearing quartz veins. It shows high light REE (LREE) [La, Ce, Pr] and lower heavy (HREE) [Er, Tm, Yb, Lu]. Positive Gd signature was observed in samples O7, O8, and O10. The concentrations of (Co+Ni+Cu+Zn)-Fe-Mn in quartz veins were plotted on a ternary diagram proposed by [17]. The diagram was used to differentiate between submarine hydrothermal and hydrogenous deposits. The data plotted indicate that the quartz veins bearing gold are of hydrothermal origin (Figure 7).

4.4. Geochemistry of Gold Bearing Soils. The results of soils analysed with instrumental neutron activation analysis (INAA) for the concentration of gold and selected major oxides and trace elements are contained in Table 5. The Fe_2O_3 content varies widely and comprise from 0.85 to 11.20 wt%. The concentration of Na_2O (<0.50 to 1.64 wt%) is generally low.

As content (<2 to 700 ppm) is noteworthy. Some of the soils are enriched in the following gold path finder elements: Sb (<2 to 12.7 ppm), W (<4 to 19 ppm), and

Table 5: Some major oxide, trace, and rare elements for concentration of soils.

(a)

Field →	Tuniya	Yar Kaura	Sado	Mayowa	Maru	Atakar	Hanudezoma	Gwar Gawo
Sample number →	S1	S2	S3	S4	S5	S6	S7	S9
Major oxide (wt.%) ↓								
Na_2O	0.06	0.07	1.67	0.07	0.17	0.42	<0.05	0.29
Fe_2O_3	2.03	1.35	9.08	11.20	0.85	8.01	2.3	2.55
Trace element (ppm) ↓								
Au (ppb)	16	<5	80	266	<5	<5	79	5700
As	127	2	16	22	3	5	121	7
Ba	300	300	800	500	400	300	400	400
Co	10	<5	71	61	<5	34	9	8
Cs	4	<2	<2	7	<2	6	4	2
Hf	16	14	5	7	11	8	10	10
Mo	<5	<5	<5	<5	<5	12	<5	<5
Rb	80	40	<30	110	<30	100	40	50
Sb	1.2	<0.2	1.9	4.2	0.3	0.7	3.1	1.4
Sc	6.6	4.4	36.1	37.1	2.4	11.4	6.4	4.3
Ta	<1	<1	<1	2	1	88	1	1
Th	9.5	7.8	1.1	4.6	5.4	8	8.3	6.4
U	4.5	3.4	<0.5	3.2	2.4	6.4	3.8	3.3
W	19	<4	<4	<4	<4	13	<4	<4
Zn	90	<50	190	250	<50	<50	<50	60
La	40	16	17	36	13	28	22	17
Ce	65	37	55	71	32	89	40	39
Nd	30	15	22	33	8	22	15	7
Sm	4.6	1.8	5.7	8	1.4	3.4	2.7	2.2
Eu	1.4	0.5	1.9	3	0.5	1	0.8	0.6
Tb	<0.5	<0.5	1.2	<0.5	<0.5	<0.5	<0.5	<0.50
Yb	4.2	2.6	5.5	5.2	1.5	2.9	2.9	1.40
Lu	0.59	0.38	0.8	0.73	0.26	0.35	0.44	0.26
ΣREE	145.8	73.28	107.9	156.93	56.66	146.65	83.84	67.46

(b)

Field →	Kadaure	Ferri Ruwa	Dangowa	Soro Kudi	Range		Mean	Standard deviation
					Min	Max		
Sample number →	S10	S11	S12	S13				
Major oxide (wt.%) ↓								
Na_2O	0.06	0.17	<0.05	0.22	<0.50	1.67	—	—
Fe_2O_3	10.4	1.16	3.72	4.12	0.85	11.2	4.73	3.84
Trace element (ppm) ↓								
Au (ppb)	2850	<5	27	<5	<5	5700	—	—
As	730	<2	33	5	<2	730	—	—
Ba	1100	600	600	400	300	1100	508.33	239.16
Br	<1	<1	7	9	<1	9	—	—
Co	237	6	12	22	<5	237	—	—
Cs	4	2	5	385	<2	385	34.92	—
Hf	6	13	15	11	5	16	10.50	3.55
Mo	<5	<5	17	<5	<5	17	—	—
Rb	130	70	110	210	<30	210	—	—
Sb	5.5	0.7	2.6	12.7	<0.20	12.7	—	—
Sc	14.8	4.1	10	16.5	2.4	37.1	12.84	11.94
Ta	<1	<1	2	66	<1	88	—	—

(b) Continued.

Field →	Kadaure	Ferri Ruwa	Dangowa	Soro Kudi	Range		Mean	Standard Deviation
					Min	Max		
Sample number →	S10	S11	S12	S13				
Th	14.6	8.6	15.5	7.1	1.1	15.5	8.08	3.95
U	6.1	3	3	3.2	<0.5	6.4	—	—
W	<4	<4	<4	<4	<4	19	—	—
Zn	140	<50	<50	<50	<50	250	—	—
La	116	19	38	21	13	116	31.92	28.03
Ce	137	41	83	45	32	137	61.17	30.44
Nd	37	16	38	14	7	38	21.42	10.79
Sm	8.5	2.2	4.8	3.6	1.4	8.5	4.08	2.34
Eu	2.2	0.7	1.3	1.1	0.5	3	1.25	0.77
Tb	<0.5	<0.5	1.4	<0.5	<0.50	1.4	—	—
Yb	4.2	2.8	4.9	3	1.4	5.5	3.43	1.36
Lu	0.63	0.41	0.69	0.45	0.26	0.8	0.50	0.18
ΣREE	305.53	82.11	170.69	88.15	56.66	305.53	123.75	69.03

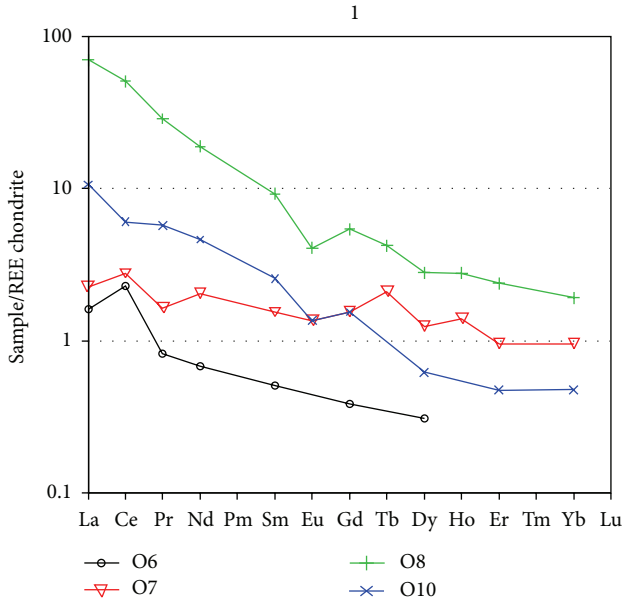

Figure 6: Chondrite normalized plots of rare earth element (REE) [16] in gold bearing quartz veins. The plot indicates negative Eu (europium) signatures for all the samples.

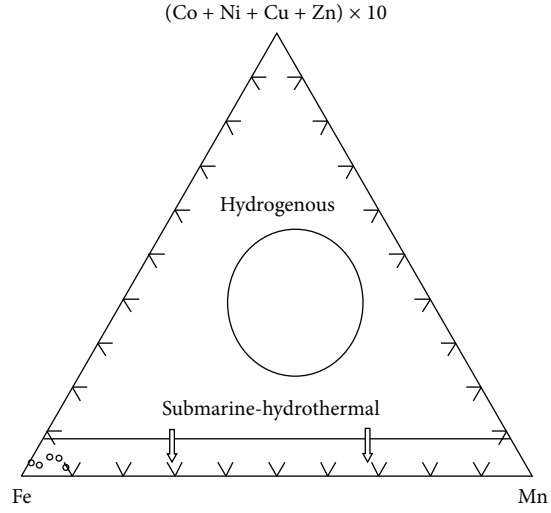

Figure 7: (Co+Ni+Cu+Zn)-Fe-Mn ternary plot of quartz veins proposed by [17] used to differentiate submarine and hydrothermal and hydrogenous deposits.

Mo (<5 to 17 ppm). The concentration of the following lithophile elements: Ba (300–1100 ppm), Cs (2–385 ppm), Hf (5–16 ppm), Sc (2.4–37.1 ppm), Th (1.1–15.5 ppm),and U (<0.50–6.4 ppm) is remarkable. Co content ranges from <5 to 237 ppm. The summation of rare earth element varies from 56.66 ppm to 305.53 ppm and is notable. The concentration of gold ranges from <5 to 5700 ppb (Table 5). The gold content in the soil samples from Gwar Gawo (5700 ppb) and Kadaure (2850 ppb) exceeded the minimum value of gold in a geomaterial (2000 ppb) that makes them to qualify as ores ([21]; Table 6). The gold content of soils from Tuniya (16 ppb), Sado (80 ppb), Mayowa (266 ppb), Hanudezoma (79 ppb), and Dangowa (27 ppb) exceeded its background values. This is a positive geochemical anomaly that indicates vertical or lateral proximity to higher grade of gold deposit. Most soil samples that have high gold content equally recorded high arsenic concentration (Figure 8). This implies that the gold occurrence or deposit is associated with arsenic (As) and could be utilized as an effective geochemical parameter to explore for gold in the study area. The concentration of antimony (Sb) (<0.20 to 12.70 ppm] is above the one in unmineralized materials (1 ppm) in most of the soils analysed. Antimony is known to associate with gold deposit, and high Sb content (12.70 ppm) of Soro Kudi field could imply proximity to gold mineralization [28].

The concentration of Hf (5 to 16 ppm) and barium (300 to 1100 ppm) exceeded its crustal abundances in all the soil

Table 6: Results of instrumental neutron activation analysis of concentration of gold in soil samples.

Sample number →	S1	S2	S3	S4	S5	S6	S7	S9	S10	S11	S12	S13
Field →	Tuniya	Yar Kaura	Sado	Mayowa	Maru	Atakar	Hanudezoma	Gwar Gawo	Kadaure	Ferri Ruwa	Dangorowa	Soro Kudi
Au (ppb) →	16	<5	80	266	<5	<5	79	5700	2850	<5	27	<5
Crustal abundance of gold (ppb) →	5	5	5	5	5	5	5	5	5	5	5	5
Clarke value (ppb) [b] →	4	4	4	4	4	4	4	4	4	4	4	4
Approximate minimum quantity to qualify as an ore (ppb) [c]	2000	2000	2000	2000	2000	2000	2000	2000	2000	2000	2000	2000

[a]: [19] and [20]; [b and c]: [21].

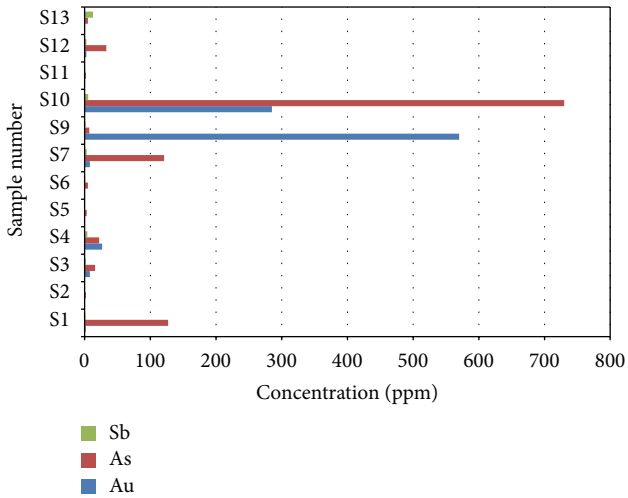

Figure 8: Bar chart of concentration of gold (Au), arsenic (As) and antimony (Sb) in soil samples retrieved from minor gold fields. The value of gold's concentration is ×10 ppm.

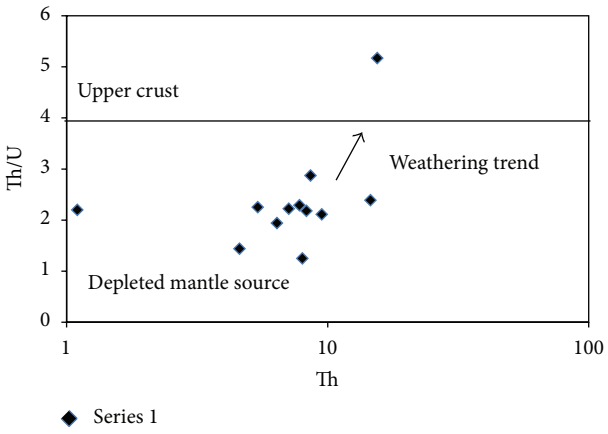

Figure 9: Plot of Th/U versus Th after [18].

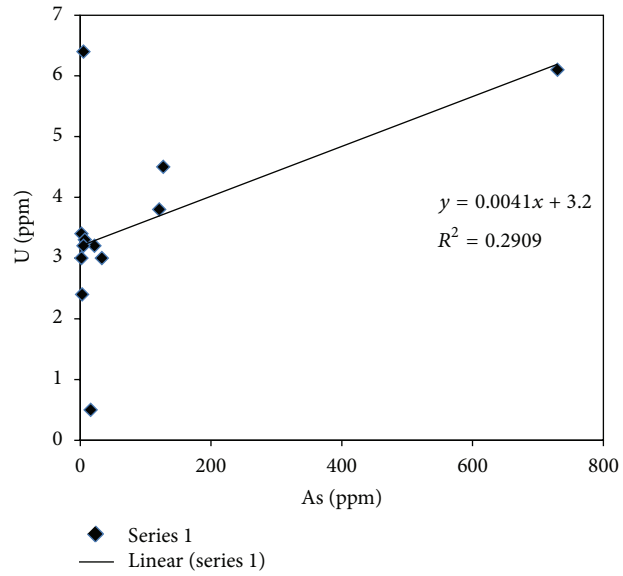

Figure 10: Plot of U versus As indicating slight positive correlation.

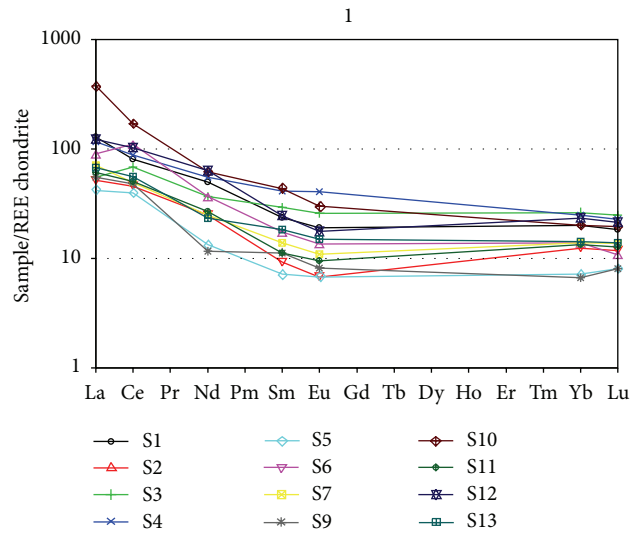

Figure 11: Chondrite normalized plots of rare earth element (REE) [16] in soil samples. Positive Eu signature was observed in samples S4 and S5. The plot indicates negative Eu (europium) signature for the other samples.

samples. The U content (<0.50 to 6.4 ppm) of most soil samples exceeded its background values. The concentration of tantalum (Ta) in soils retrieved from Atakar (S6) is 88 ppm and is above its crustal abundance of 2 ppm. This could indicate nearness to tantalum (Ta) occurrence. The Th/U ratio ranges from 1–3 and it indicates weak weathering. It shows Th/U ratio like the depleted mantle (Figure 9). Plot of U versus As is positive with correlation coefficient (R^2) = 0.30 (Figure 10). The Pearson correlation coefficient computed with Minitab statistical software was used to establish the relationship between gold and other parameters analysed. The relationship between Fe_2O_3 and Au is weak positive correlation. The relationship between Na_2O and Au is very weak negatively correlated.

Strong positive correlation exists between Au with Ba, Co and La. The relationship between Au with Cr, Th, U, Zn, Ce and Sm is very weak positively correlated.

Strong negative correlation exist between Au with Hf, Au with Yb and Au with Lu. The correlation relationship between Au with the following elements: Br, Cs, Mo, Rb, Sb, Sc, Ta, W, Nd, Eu and Tb is very weak negative.

Very strong positive correlation exists between the following pairs of elements Co and As, La and Co, Ce and Co, Cs and Sb, Sb and Rb, Sc and Eu, Zn and Sm, Zn and Eu, La and Ce, Ce and Nd, Nd and Sm, Nd and Yb, Sm and Eu, Sn and Lu, Eu and Yb, Eu and Lu, and Yb with Lu.

Figure 11 illustrates chondrite normalized plots of rare earth element (REE) [16] in soils. It shows highly enriched chondrite normalized LREE and MREE ($[La/Sm]_N$ about 1.88 to 8.58) and lower flat heavy (HREE). Some samples indicate

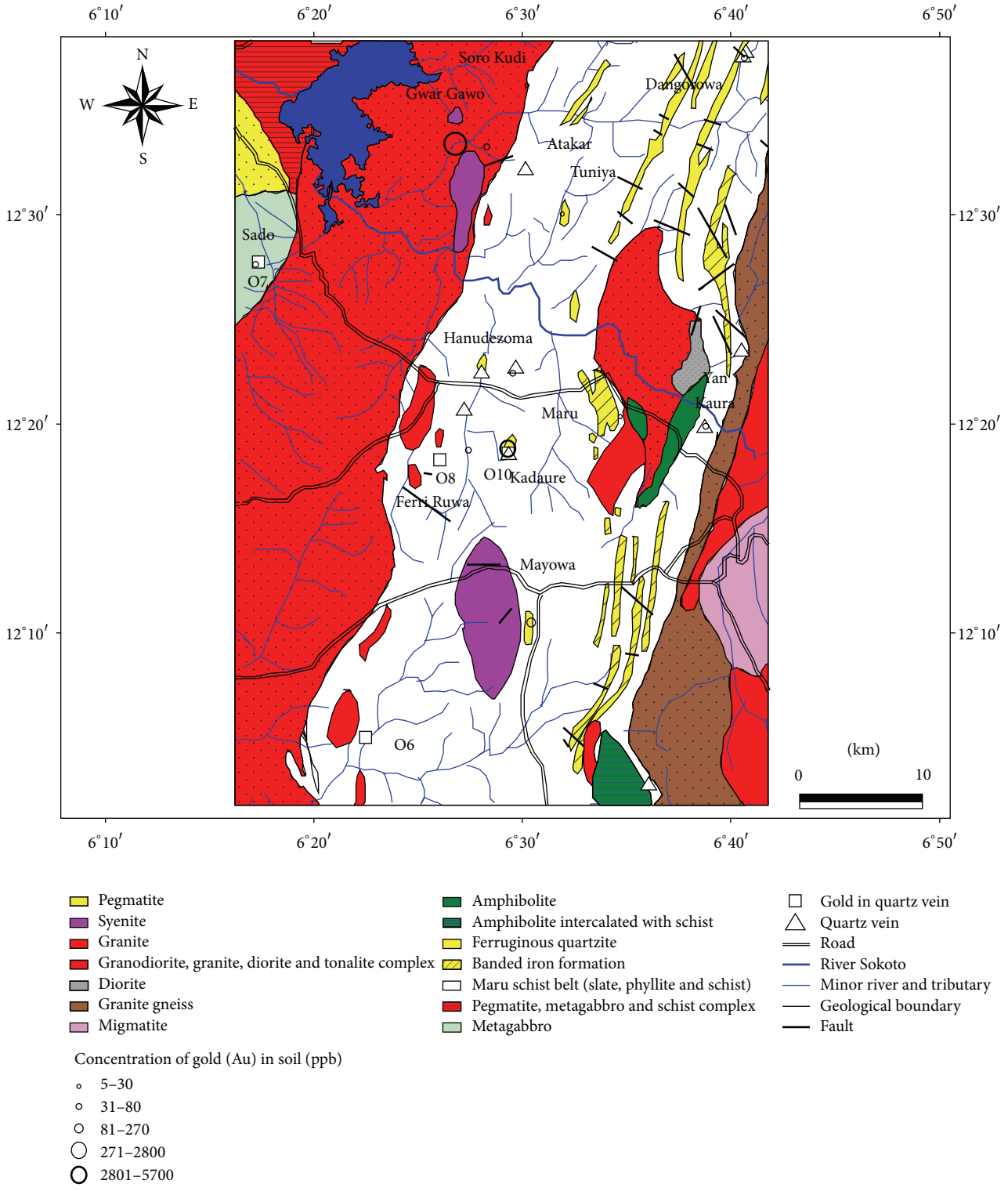

FIGURE 12: Geological map of the study area showing locations of gold bearing quartz veins and concentration of gold in soil samples.

positive anomalies for Ce (S6 and S3), Eu (S4 and S5) with Lu (S9 and S5). The soils displayed pronounced negative Pr and Nd anomalies. Significant gold anomalies in soil occur at Gwar Gawo (5700 ppb), Kadaure (2850 ppb), and Mayowa (266 ppb) (Figure 12). Considerable anomalies of antimony occur at Soro Kudi (12.7 ppm), Kadaure (5.5 ppm), and Mayowa (4.2 ppm). Substantial anomalies of arsenic occur in Tuniya (127 ppm), Hanudezoma (121 ppm), and Kadaure (730 ppm) (Figure 13). Distinct anomalous uranium content was recorded at Atakar (6.4 ppm) and Kadaure (6.1 ppm).

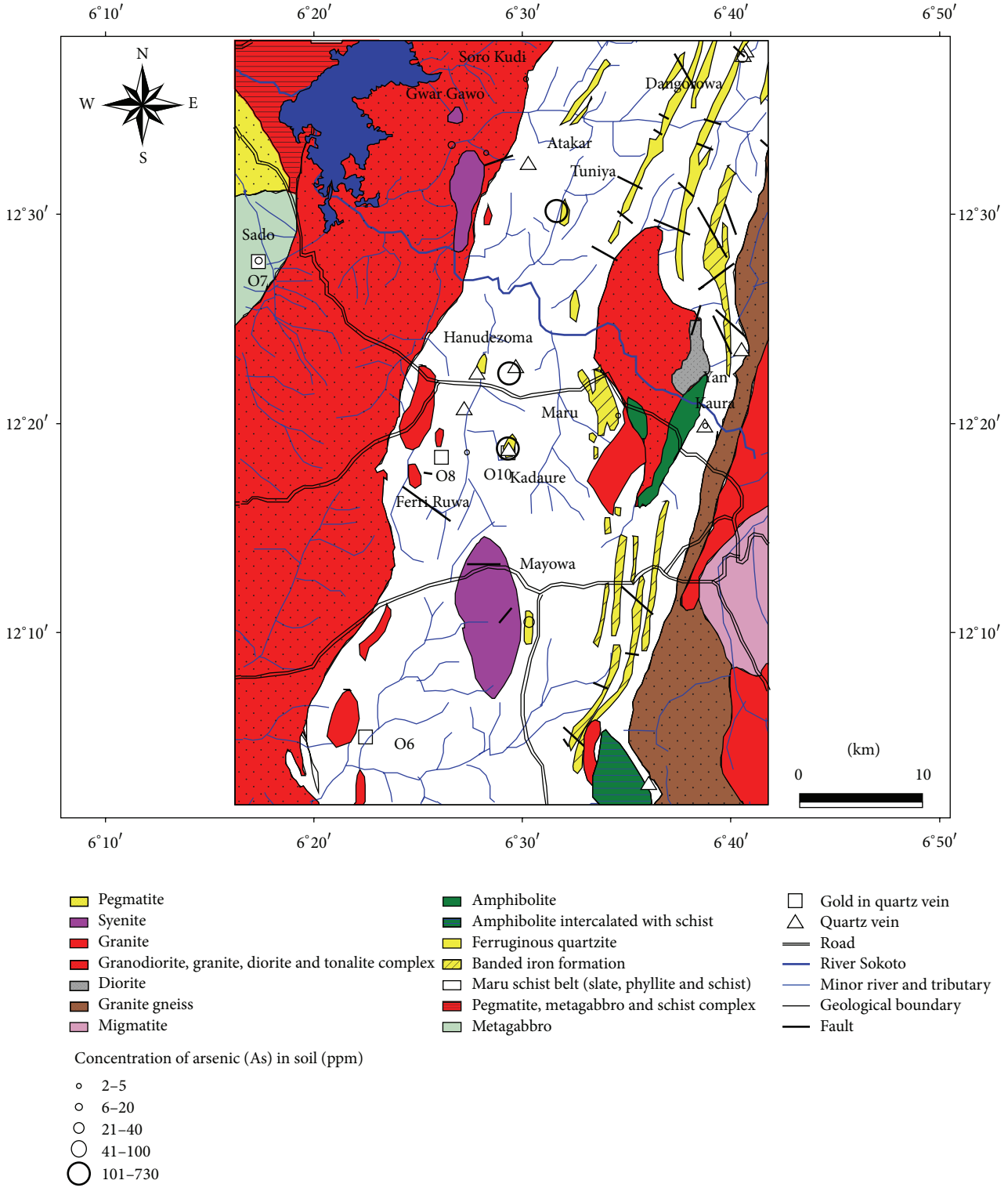

FIGURE 13: Geological map of the study area showing locations of gold bearing quartz veins and concentration of arsenic in soil samples.

Field and petrographic evidences at Maru schist belt area indicate the occurrence of gold bearing quartz veins and soils within sealed fractures hosted by slate, phyllite, schist, and metagabbro. Several granitic, granodioritic, tonalitic, dioritic and syenitic intrusions close to the quartz veins and minor gold field soils were observed (Figures 12 and 13). Similar observation was discovered at Bini Yauri and [29] suggested that magmatic fluid or recirculated groundwater may be

part of the ore constituents at some stage of vein evolution and accompanied alteration. There are very few auriferous Archean greenstone belts or productive Phanerozoic orogens that contain gold provinces without nearby intrusions of roughly the same age. Whether or not any of these igneous bodies are the source of fluids and metals that become a part of the gold-forming systems is often a highly debated issue; the other obvious scenario is that both melts and fluids may be products of the same deep-crustal or even mantle-generated, thermal event [30].

Anomalous gold content in soil occurs close to syenite plutons in Gwar Gawo (5700 ppb) and Mayowa (266 ppb) minor gold fields (Figure 12). This suggests the possibility of magmatism as the source of mineralizing fluids. Dangorowa, Tuniya, Kadaure, and Mayowa minor gold fields are closely associated with ferruginous quartzites. Soro Kudi field is situated on the contact boundary between granodiorite, granite, diorite, and tonalite complex within Maru schist belt. The proximity of strike-slip faults to Atakar, Dangorowa, Ferri Ruwa and Mayowa is noteworthy and could have served as the conduit for gold mineralizing fluid (Figure 13 and [31]. A multidataset analysis of selected parts of the study area provided useful information and metallogenic models that can assist in gold exploration and recovery [32, 33]. Figures 12 and 13 show the application of gold mineralization model criteria that integrated digital geochemical (gold and arsenic concentration in quartz veins and soils) and strike slip fault data. Areas favourable or that indicate gold mineralization are identified on the basis of combination of the various elements of the model in the following decreasing order of weightings: gold in quartz vein, gold in soil, concentration of arsenic in quartz vein with soil, level of antimony in soil and proximity to fault. Based on the aforementioned criteria, the prospectivity of the minor gold field ranking in decreasing order is Kadaure > Sado > Mayowa > Hanudezoma > Ferri Ruwa > Gwar Gawo > Dangowa > Tuniya > Soro Kudi > Atakar. Yar Kaura and Maru fields displayed the least geochemical and structural criteria used in prospectivity ranking (Figures 12 and 13).

5. Conclusions

Based on field, petrographic, and geochemical evidences, the ore fluid may have been derived largely from fracturing, metamorphic dewatering [29] and crustal devolatilization [30] of sedimentary and gabbroic protolith of the host rocks. Isotopic studies of fluid components of the quartz veins will further confirm the propose origin.

The emplacement of the quartz vein is associated with D_2 deformation as indicated by similarity in the generalized strike direction of quartz vein and host rocks. It postdates regional metamorphism and fracturing. These structural settings suggest that the emplacement of gold mineralization occurred during Late Pan African orogeny [34]. Appreciable As signature further confirms that the quartz veins were formed in an orogenic setting [35]. Eluvial gold occurrence resulted from residual weathering of gold bearing quartz veins.

Conflict of Interests

The authors declare that there is no conflict of interests regarding the publication of this paper.

Acknowledgments

The study is part of the first author's Ph. D. research supervised by Professor A. F. Abimbola at the Department of Geology, University of Ibadan, Nigeria. The support rendered by Dr. Thomas Oberthur of BGR (Federal Institute of Geosciences and Natural Resources, Hannover, Germany) in the course of the research is gratefully acknowledged. The efforts of Dr. Frank Melcher of BGR and Andreas Wilms are appreciated. The authors are very grateful to Detlef Reguard of BGR who performed all wave length dispersive X-ray fluorescence analysis. Thanks goes to Martin Klocke and Mostafa for their numerous supports. The help rendered by the following BGR scientists is appreciated: Jerzy Lodziak, Dr. Maria Alexandrovna Sitnikova, Henry Donald, and Mr. Andreas Schneibner.

References

[1] J. F. Truswell and R. N. Cope, *The Geology of Parts of Niger and Zaria Provinces, Northern Nigeria*, Geological Survey Nigeria Bulletin no. 29, 1963.

[2] M. Woakes and B. E. Bafor, "Primary gold mineralization in Nigeria," in *GOLD 1982: The Geology, Geochemistry and Genesis of Gold Deposits*, R. P. Foster, Ed., Geological Society of Zimbabwe Special Publication no. 1, Balkema, Rotterdam, The Netherlands, 1983.

[3] K. P. C. J. D'Souza, U. A. Danbatta, and P. S. Newall, "Comprehensive solid minerals resource survey and assessment," Tech. Rep., Wardell Armsstrong, 2005.

[4] F. R. Siegel, *Applied Geochemistry*, John Wiley & Sons, New Jersey, NJ, USA, 1974.

[5] A. G. Darnley, B. Björklund, N. Gustavsson et al., *A Global Geochemical Database for Environmental and Resource Management: Recommendations for International Geochemical Mapping Final Report of IGCP Project 259*, 1995.

[6] R. W. Boyle, *The Geochemistry of Gold and Its Deposits*, Geological Survey of Canada Bulletin 280, 1979.

[7] J. C. Antweiler and W. L. Campbell, "Gold in exploration geochemistry," in *Precious Metals in the Northern Cordillera*, vol. 10, pp. 33–44, The Association of Exploration Geochemists, 1982.

[8] J. A. Adekoya, *The geology of banded iron formation in the Precambrian basement complex of northern Nigeria [Ph.D. thesis]*, University of Ibadan, Ibadan, Nigeria, 1991.

[9] A. E. O. Ogezi, "Origin and Evolution of the Basement Complex of North-Western Nigeria in the light of new Geochemical and Geochronological Data," in *Precambrian Geology of Nigeria*, Geological Survey of Nigeria, Ed., pp. 301–312, Esho, Kaduna, Nigeria, 1988.

[10] J. A. Adekoya, "The geology and geochemistry of the Maru banded Iron-Formation, Northwestern Nigeria," *Journal of African Earth Sciences*, vol. 27, no. 2, pp. 241–257, 1998.

[11] R. Holt, I. G. Egbuniwe, W. R. Fitches, and J. B. Wright, "The relationships between low-grade metasedimentary Belts, calc-alkaline volcanism and the Pan-African orogeny in N-W Nigeria," *Geologische Rundschau*, vol. 67, no. 2, pp. 631–646, 1978.

[12] A. C. Ajibade and W. R. Fitches, "The Nigerian precambrian and the Pan-African orogeny," in *Precambrian Geology of Nigeria*, P. O. Oluyide, W. C. Mbonu, A. E. O. Ogezi, I. G. Egbuniwe, A. C. Ajibade, and A. C. Umeji, Eds., pp. 45–53, Geological Survey of Nigeria Publication, 1988.

[13] P. O. Oluyide, "Structural trends in the Nigerian basement complex," in *Precambrian Geology of Nigeria*, P. O. Oluyide, W. C. Mbonu, A. E. Ogezi, I. G. Egbuniwe, A. C. Ajibade, and A. C. Umeji, Eds., pp. 93–98, Geological Survey of Nigeria Publication, 1988.

[14] A. Miyashiro, *Metamorphic Petrology*, Oxford University, Oxford, UK, 1994.

[15] S. A. Oke, *Petrogenesis, structural characteristics of Precambrian rocks with associated copper and gold mineralization in parts of Gusau area, Northwestern Nigeria [Ph. D. Thesis]*, University of Ibadan, Ibadan, Nigeria, 2014.

[16] W. V. Boynton, "Cosmochemistry of the rare earth elements: meteorite studies," in *Rare Earth Element Geochemistry*, P. Henderson, Ed., pp. 63–114, Elsevier, Amsterdam, The Netherlands, 1984.

[17] E. Bonatti, T. Kraemer, and H. Rydell, "Classification and genesis of submarine iron-manganese deposits," in *Proceedings of the Conference on Ferromanganese Deposits on the Ocean Floor*, D. R. Horn, Ed., pp. 149–166, Arden House, Harriman, NY, USA, 1972.

[18] S. M. McLennan, S. Hemming, D. K. McDaniel, and G. N. Hanson, "Geochemical approaches to sedimentation, provenance, and tectonics," *Special Paper of the Geological Society of America*, vol. 284, pp. 21–40, 1993.

[19] J. Green, "Geochemical table of the elements for 1959," *Bulletin of the Geological Society of America*, vol. 70, no. 9, pp. 1127–1184, 1959.

[20] S. R. Taylor and S. M. McLennan, *The Continental Crust: Its Composition and Evolution*, Blackwell, Oxford, UK, 1985.

[21] J. M. Guilbert and C. F. Park, *The Geology of Ore Deposits*, W. H. Freeman, New York, NY, USA, 1986.

[22] Actlab, *Analytical Methods for Activation Laboratory*, 2012, http://www.actlabsint.com/.

[23] E. L. Hoffman, "Instrumental neutron activation in geoanalysis," *Journal of Geochemical Exploration*, vol. 44, no. 1–3, pp. 297–319, 1992.

[24] M. G. Best, *Igneous and Metamorphic Petrology*, Blackwell Science, 2nd edition, 2003.

[25] A. A. Surour, A. A. El-Kammar, E. H. Arafa, and H. M. Korany, "Dahab stream sediments, southeastern Sinai, Egypt: a potential source of Gold, magnetite and zircon," *Journal of Geochemical Exploration*, vol. 77, no. 1, pp. 25–43, 2003.

[26] A. Mücke, "The Nigerian manganese-rich iron-formations and their host rocks—from sedimentation to metamorphism," *Journal of African Earth Sciences*, vol. 41, no. 5, pp. 407–436, 2005.

[27] J. R. Craig and D. J. Vaughan, *Ore Microscopy and Ore Petrography*, John Wiley & Sons, 2nd edition, 1996.

[28] P. M. Ashley, D. Craw, B. P. Graham, and D. A. Chappell, "Environmental mobility of antimony around mesothermal stibnite deposits, New South Wales, Australia and Southern New Zealand," *Journal of Geochemical Exploration*, vol. 77, no. 1, pp. 1–14, 2003.

[29] S. O. Akande, O. Fakorede, and A. Mucke, "Geology and genesis of gold-bearing quartz veins at Bini Yauri and Okolom in the Pan-African domain of Western Nigeria," *Geologie en Mijnbouw*, vol. 67, no. 1, pp. 41–51, 1988.

[30] R. J. Goldfarb, T. Baker, B. Dube, D. I. Groves, C. J. R. Hart, and P. Gosselin, "Distribution, character and genesis of gold deposits in metamorphic terranes," in *Economic Geology 100th Anniversary Volume*, pp. 407–450, Society of Economic Geologists, Littleton, Colo, USA, 2005.

[31] V. M. Kreiter, *Geological Prospecting and Exploration*, Mir, Moscow, Russia, 1968.

[32] J. A. Plant, A. Gunn, M. Holder et al., "Multidataset analysis for the development of gold exploration models in Western Europe," British Geological Survey Report SF/98/1, 1998.

[33] W. Hatton, T. Colman, D. Cooper, A. Gunn, and J. A. Plant, "Mineral exploration and information technology," in *Proceedings of the Minerals, Land and Natural Environment Conference*, pp. 41–63, Institution of Mining and Metallurgy, 1998.

[34] E. O. Wuyep, I. Garba, and P. A. Onwualu, "Review of structures, fluid flow and gold deposits in Nigeria," *Geological Society of America Abstracts*, vol. 39, no. 6, p. 623, 2007.

[35] F. Robert, R. Brommecker, B. F. Bourne et al., "Models and exploration methods for major gold deposit types," in *Proceedings of the 5th Decennial International Conference on Mineral Exploration (Exploration '07)*, B. Milkereit, Ed., pp. 691–711, 2007.